Aerosol and Air Quality Research, 12: 409–419, 2012

ISSN: 1680-8584 print / 2071-1409 online
doi: 10.4209/aaqr.2011.08.0134

Antibacterial and Regenerated Characteristics of Ag-zeolite for Removing Bioaerosols in Indoor Environment

Hsin-Han Cheng[1], Chu-Chin Hsieh[2*], Chia-Hsi Tsai[2]

[1] *Graduate School of Engineering Science and Technology, National Yunlin University of Science and Technology, Touliu, Yunlin, Taiwan*
[2] *Department of Environmental and Safety Engineering, National Yunlin University of Science and Technology, Touliu, Yunlin, Taiwan*

ABSTRACT

The antibacterial reaction rate k_t (CFU/g-hr) and total antibacterial capacity q_T (CFU/g) were calculated to evaluate the performance of antibacterial Ag-zeolite (AgZ) with a series of experiments. The continuous antibacterial reactions at 10 and 80 hr were respectively repeated nine times to evaluate the AgZ antibacterial ability. An antibacterial system was conducted in a fixed bed reactor packed with AgZ to reduce bacterium and fungus counts in the indoor environment. The AgZ used in this study was prepared in two steps including Y-type zeolites synthesis and Ag ion-exchange. X-ray diffraction (XRD) and field emission scanning electron microscopy (FE-SEM) were carried out to identify the characteristic of AgZ. The results demonstrated that the antibacterial efficiencies of 1, 2 and 3 wt% AgZ against bacterium and the fungus were all higher than 95% after 120 min of operation, and 1 wt% AgZ was considered to be more cost-effective since its antibacterial efficiency could approach 90% in less than 60 min. The 1 wt% AgZ had excellent performance repeated usage up to nine times.

Keywords: Bacterium; Fungus; Antibacterial reaction rate; Antibacterial capacity; Regeneration.

INTRODUCTION

Indoor air quality (IAQ) is an increasingly important issue for human health due to people spending 90% of their life indoors (Reynolds *et al.*, 2001; Tringe *et al.*, 2008). Most indoor environments use air conditioners to control the temperature and humidity. A reduction in the ventilation rate could achieve potential energy savings. On the other hand, continuing running the system for a long time decreases the efficiency of air ventilation and causes bioaerosols, airborne particles of biological origins, to accumulate indoors (Lee, 2011). Bioaerosols contribute to about 5–34% of indoor air pollution (Srikanth *et al.*, 2008), including viruses, bacteria, fungi and all varieties of living materials with highly variable and complex characteristics. Unfortunately, high bioaerosol concentration exposure is often associated with sick building syndrome (SBS) and hypersensitivity diseases (Main, 2003; Lee *et al*., 2011).

UV irradiation, electric ion emissions and heating ventilation air conditioning (HVAC) systems are the most common control methods for removing aerosol pollutants in residential and commercial buildings. UV irradiation is known to have a removal effect on the bioaerosols and it can be applied by a simple installation (Nicas and Miller, 1999; Lin and Li, 2002; Grinshpun *et al.*, 2007), but the UV irradiation may produce ozone and radicals cause harmful effects to humans (Duthie *et al.*, 1999). Although air electric ions can remove indoor aerosol particles (Huang *et al.*, 2008), the shortcomings of producing ozone and the resulting electric charges accumulating on surrounding surfaces need to overcome (Phillips *et al.*, 1999). HVAC systems can remove or dilute more than 80% of aerosols or moisture from the outdoors, but they can also provide a favorable environment for bioaerosols to grow as ventilation or air conditioning systems are usually equipped with low efficiency filters (Jung *et al.*, 2006; Ji *et al.*, 2007; Huang *et al.*, 2008; Kim *et al*., 2011; Kwon *et al*., 2011).

Currently, nano-materials have become the most widely used agent to reduce indoor bioaerosols (Paschoalino and Jardim, 2008). The typical nano-materials used include heavy metals or ions such as silver, zinc and copper. Compared with other antibacterial heavy metals, silver particles and silver ions are relatively less toxic to human cells (Russell and Hugo 1994) and have strong activity to control bacterial growth at low concentrations (Feng *et al.*, 2000; Kawahara *et al.*, 2000; Inoue *et al.*, 2002). Because of the antibacterial activity of silver, many silver-containing materials have been developed for antibacterial applications (Jeon *et al.*, 2003;

* Corresponding author. Tel.: +886 5 5342601;
Fax: +886 5 5312069
E-mail address: hsiehcc@yuntech.edu.tw

Zhang *et al.*, 2004; Morrison *et al.*, 2006; Wang *et al.*, 2006). Zeolite is one of the nano-materials with several advantages such as selective adsorption, hydrophobic characteristic, multiporous structure, plasticity, and regeneration. Coating or impregnating zeolite with metallic silver (Ag) particles to prepare zeolite composites can enhance the antibacterial ability of materials, and these materials can inhibit bacterial growth effectively.

Most of current antibacterial studies have focused on microorganisms in liquid phases such as using the methods of growth inhibition, minimum inhibitory concentrations and zone of inhibition assays to determine the antibacterial properties of materials (Cinar *et al.*, 2009; Park *et al.*, 2009; Mohan *et al.*, 2011; Wu *et al.*, 2011). There is lack of information about investigating air phase bioaerosol removal systems in a continuous-flow environment. In this study, a better reservoir of Y-type zeolite was used because of its relatively high ion exchange capacity and lattice stability (Inoue *et al.*, 2008; Zhang *et al.*, 2008; Dastanian and Seyedeyn-Azad, 2010; Talebi *et al.*, 2010). Ag-zeolite (AgZ) composites were prepared and applied in an antibacterial system to reduce indoor bacterial and fungus counts. Furthermore, it is necessary to find adequate and practical parameters for controlling bioaerosols in indoor environments. The objectives of this work are to prepare AgZ and apply it in a series of antibacterial and regenerated experiments under the continuous-flow conditions. The bioaerosol antibacterial efficiencies, antibacterial reaction rate k_t (CFU/g-hr) and total antibacterial capacity q_T (CFU/g) of AgZ are investigated.

MATERIALS AND METHODS

Materials

Sodium silico-aluminate, silics and sodium hydroxide powder were used to synthesize zeolite. Sodium silico-aluminate (Grade Z-14, Grace Davison Division) purchased from WR Grace & Co. Company was used as the aluminate source of zeolite. Silics (Hi-SilTM 238, SiO_2 molecular weight 60.1 g/mole, CAS Number 7631-86-9) purchased from PPG Industries Taiwan Ltd. was used as the silica source of zeolite. Sodium hydroxide powder (> 97 wt %) was purchased from Katayama Chemical Co., Ltd. Silver nitrate $AgNO_3$ purchased from Katayama Chemical Co., Ltd. was used in preparation of AgZ. Nutrient agar and malt extract agar (Difco™ & BBL™ Manual) were used for the cultivation of the bacterium.

Preparation of the AgZ

The antibacterial materials AgZ were prepared in two steps including Y-type zeolites synthesis and Ag ion-exchange. The detailed preparation is described in the following sections.

Synthesis Zeolites

A hydrothermally synthesized method was used for Y-type zeolite synthesis. The sodium aluminate and silica precursors for Y-type zeolite were prepared by the dissolution of NaOH and deionized water. The colloidal mixer was obtained by stirring these precursors thoroughly. The colloidal mixer was prepared and proceeded to produce hollow columns (5 mm ϕ × 1 mm id. × 3 mm L) by extrusion. After centrifuging for 3 hr, washing with deionized water, air drying at 105°C for 8 hr, and calcinating under 450°C for 8 hr, the reservoir zeolite was obtained.

Ion-exchange and Calcination

The silver-coated zeolite was prepared by the ion-exchange method. The ion-exchange was carried out by the addition of 10 g zeolite into adequate concentrations of silver nitrate solutions to prepare 1, 2 and 3 wt% AgZ. The suspension was stirred at room temperature in the dark for 24 hr. Then centrifuged (3 hr) and washed with deionized water to remove excess $AgNO_3$, sequentially. AgZ was obtained after air drying under 105°C for 8 hr and calcinating under 450°C for 8 hr.

Material Characterization

X-ray diffraction (XRD) was carried out to identify the phase structure of antibacterial materials. The XRD patterns were obtained with 2θ angle scanning from 20 to 50°. Field emission scanning electron microscopy (FE-SEM, Joel 5410LV) was carried out to examine the morphological properties of the AgZ. The nitrogen absorbance method using a multipoint BET technique (ASAP 2010, Micrometritics, USA) was carried out to analyze the Brunauer-Emmett-Teller specific surface area (S_{BET}) and pore size distributions of antibacterial materials.

Antibacterial Experiments

Antibacterial System

The antibacterial experiment conditions and background information is shown in Table 1. The laboratory-scale experiments were carried out in-situ with room volume of 100 m^3 (5 m L × 5 m W × 4 m H) with plaster walls. Evaluation of the AgZ performance was conducted by measuring the single-pass efficiency in reducing concentrations of bacterium and fungus. An antibacterial system was used to reduce bacterium and fungus counts in the indoor environment, and the flow chart of the antibacterial process is shown in Fig. 1. The main body of the antibacterial system is a fixed bed reactor (2 cm id. × 30 cm L) packed with 10 g antibacterial material and the system is integrated with a pre-heated device which could offer 2 hr at 150 ± 5°C heat for material regeneration. The fixed bed was filled with 5 mm glass beads in order to provide a uniform flow of air flow through the fixed bed. The AgZ material was reused nine times (regenerated eight times), and the materials were assigned to Fresh, Run 2, Run 3, Run 4, Run 5, Run 6, Run 7, Run 8 and Run 9 (Run 2 indicated that the AgZ was used a second time). The air flow rate was controlled by using an air pump (Lamotte Chemical Products Co., Chestertom, MD). The continuous experiments performed under system air flow rates were controlled at 100 L/min for antibacterial processes and 1 L/min for material regeneration. The air was flowed in the reverse direction during the regeneration process. Temperature and humidity during each antibacterial experiment were 25 ± 2°C and 55 ± 5%, respectively. The

Table 1. Conditions of antibacterial experiments.

Conditions of antibacterial experiments	Values
Environmental conditions:	
Room volume (m^3)	100 (5 m L × 5 m W × 4 m H)
Bacterium concentration in the influent (CFU/m^3)	1,311 ± 368 (N = 45)
Fungus concentration in the influent (CFU/m^3)	1,049 ± 299 (N = 45)
Temperature (°C)	25 ± 2
Relative humidity (%)	55 ± 5
Equipment conditions:	
Packed column size (cm)	30 cm L, id. 2 cm
AgZ packed in fixed bed (g)	10
Pre-heated temperature (°C)	150 ± 5
AgZ regeneration time (hr)	2
Air pump and sampling flow rates (L/min)	100
Bioaerosol sampling volume (L)	15
Sampling period for a cycle (hr)	10 or 80

CFU/m^3: colony forming units per cubic meter.

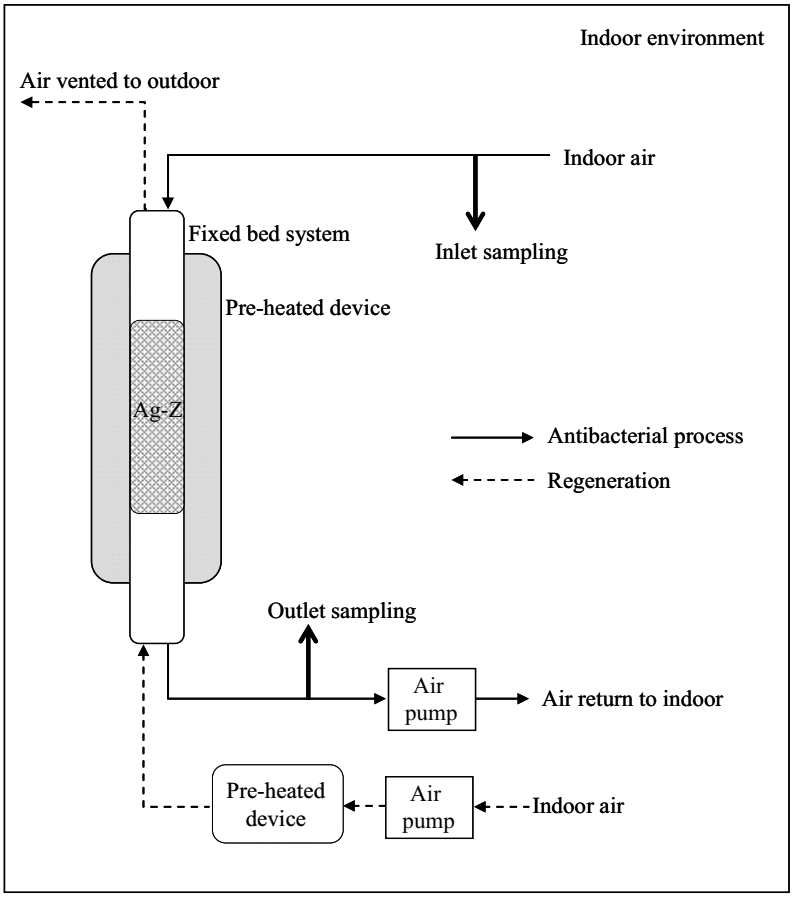

Fig. 1. Schematic of the fixed bed system.

repeatedly used materials were applied in the antibacterial experiment, and the antibacterial efficiency and total antibacterial capacity of each cycle was calculated by analyzing the bacterial and fungal counts.

Sampling

The inlet and outlet sampling port of the antibacterial system were analyzed and the field blanks were also analyzed exactly using the same method. The bioaerosol concentration was expressed in colony forming units per cubic meter (CFU/m^3). Bacterium and fungus were collected using an Andersen biological cascade impactor (Andersen Sampler, Inc., Atlanta, Ga.) at an air flow rate of 100 L/min (sampling volume 15 L), and it conformed to isokinetic sampling conditions. The experiments sampling period for an antibacterial cycle was 10 and 80 hr. Before sampling,

the tubes and pipes of Andersen Sampler were washed with ethanol and deionized water.

Microbial Analysis Methods

The cultivation and determination of bacterium and fungus were determined by the standard methods of the Taiwan EPA NIEA E301.11C and NIEA E401.11C, respectively, to assess biological contaminants in the indoor environment. Both methods referred to the US EPA standard method of "Guidelines for the assessment of bioaerosols in the indoor environment". The reported data was the average value of two parallel samples. Petri dishes were incubated 48 ± 2 hr at 30 ± 1°C and 5 ± 2 days at 25 ± 1°C for bacterial counts and for fungal counts, respectively.

Calculation

The antibacterial reaction rate (k_t) at time t of AgZ was defined by Eq. (1) as the amount of microbial counts removed per g of AgZ and per unit time:

$$k_t = \frac{(C_0 - C)Q}{M_Z} \quad (1)$$

The total antibacterial capacity (q_T) of AgZ was calculated from Eq. (2):

$$q_T = \frac{\sum (C_0 - C)Q\Delta t}{M_Z} \quad (2)$$

where k_t is the antibacterial reaction rate of AgZ (CFU/g-hr) at time t; q_T is the total antibacterial capacity of AgZ (CFU/g) during the operation time; C_0 and C are inlet and outlet bioaerosol concentrations of the fixed bed system (CFU/m^3); Q is the inlet air flow rate (m^3/min); Δt is the time difference between two influent sampling times (min); M_z is the AgZ mass used in the antibacterial experiment (g).

RESULTS AND DISCUSSION

Structural Characterization

AgZ was prepared as hollow columns (5 mm ϕ × 1 mm id. × 3 mm L) by extrusion. AgZ applied in air conditioners could reduce high pressure drops, and it could achieve energy savings and reduce electricity usage. Fig. 2 shows the XRD patterns of the zeolite and AgZ composites. The typical diffraction peaks of zeolite ranged from 2θ of 10 to 35°, and their intensity decreased when the increasing Ag content slightly. The prominent peaks of Ag at 2θ values of about 38, 44, 65, and 77° represented the (111), (200), (220), and (311) Bragg's reflections of face-centered cubic crystalline silver, and this result further confirmed a previous study (Khanna *et al.*, 2005). Moreover, increasing the amount of Ag in the zeolite led to the enhancement of the characteristic peaks of Ag, implying the development of crystalline Ag nano-particles. SEM was used to evaluate the surface morphology of the AgZ. As shown in Fig. 3(a), the surface of pure zeolite looked very satiny in appearance. The surfaces of the 1 wt% AgZ (Fig. 3(b)) exhibited a rough homogeneous morphology, which means that the zeolite

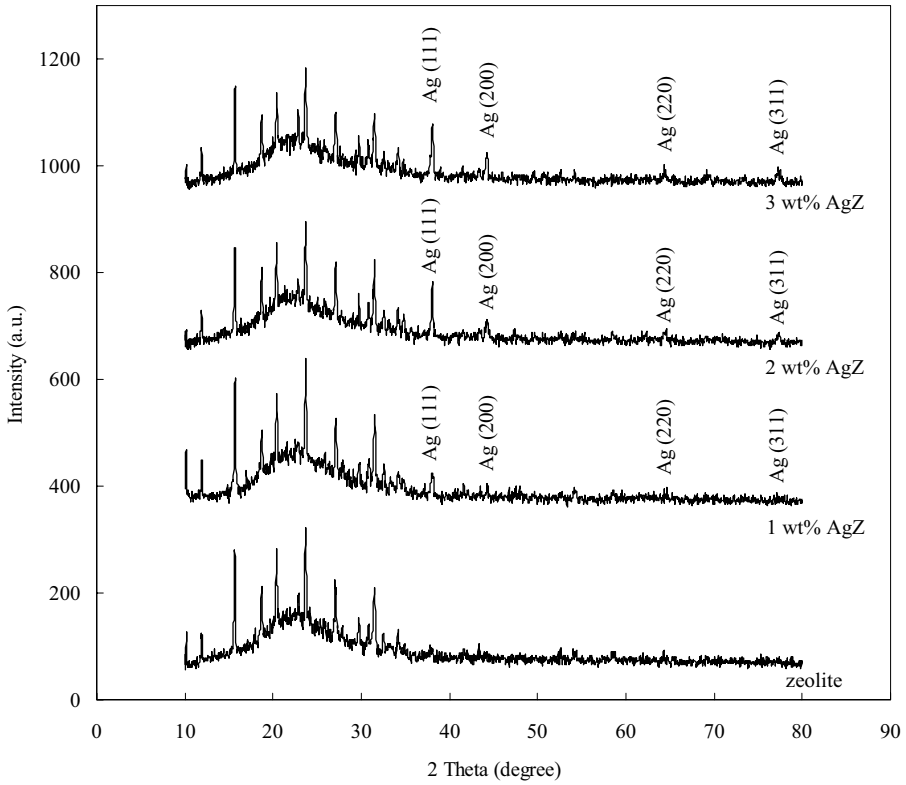

Fig. 2. XRD patterns of the zeolite composites.

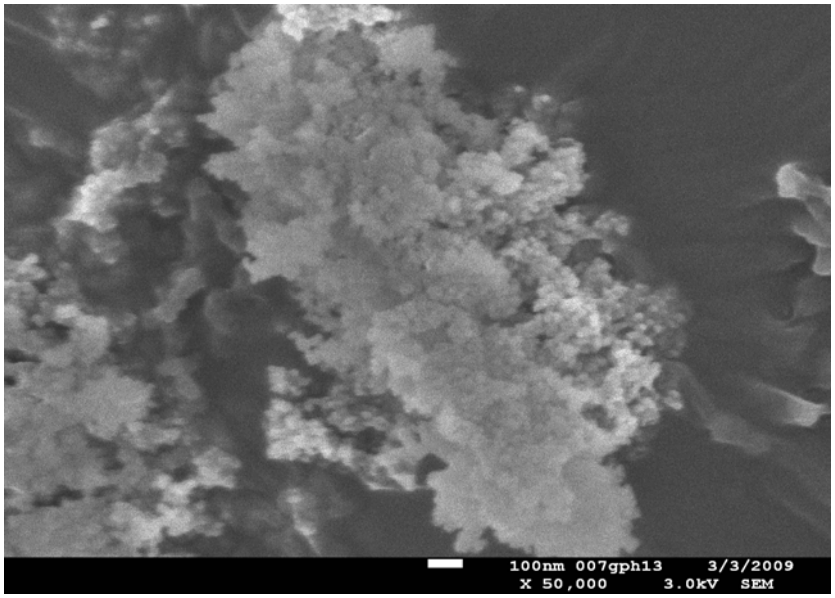

(a)

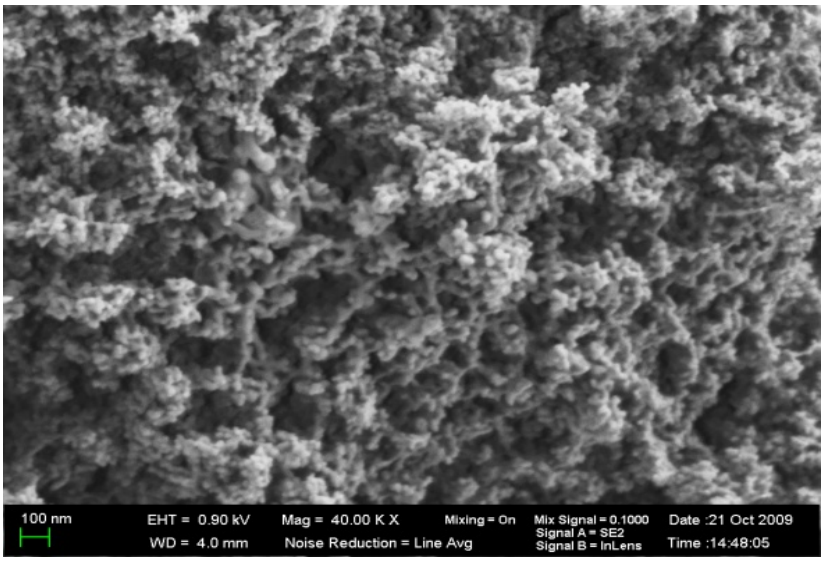

(b)

Fig. 3. FE-SEM images of (a) zeolite (× 50,000) and (b) 1wt% AgZ (× 40,000).

surfaces were covered with grafted Ag particles. It was observed that the AgZ composites consisted of nano-agglomerated (typically in the range of less than 100 nm) and uniformly distributed Ag particles in the zeolite. Moreover, zeolites are aluminosilicate solids with structures based upon a three dimensional framework and they have micropores constructed by connecting many small cages. Silver ions are located at specific positions within the interior of the cage because of the surrounding electron density (Kawahara *et al.*, 2000; Inoue *et al.*, 2002; Thom *et al.*, 2003). Because the native cations in the zeolite structure can be exchanged with metal ions, zeolite is one of the superior reservoirs for coating metal catalysts, (Ruihong *et al.*, 2006).

AgZ was recycled nine times in the study, and the S_{BET} values and pore diameter distributions were analyzed for Fresh, Run 6 and Run 9 AgZ. As shown in Table 2, Zeolite had a S_{BET} value of 257 m^2/g, and 1 wt% AgZ had lower S_{BET} of 216 m^2/g due to the blocking of Ag particles deposited into zeolite channels and the channel structures had not significantly changed. The S_{BET} values of Fresh, Run 6 and Run 9 AgZ were 216, 115 and 106 m^2/g, respectively. S_{BET} decreased with regeneration times probably due to the partial collapse of the channels by the 150°C heating process. However, Run 6 and Run 9 AgZ had the approximate S_{BET}, and it might be that the channel structure of AgZ had not significantly changed after six usages. The pore diameter distribution of 1 wt% AgZ (74% particle size was 20–80 nm) was similar to zeolite (78% particle size was 20–80 nm). AgZ used the sixth time had higher pore diameter size, and the primary particle size of it was 20–80 nm (30%) and over 80 nm (61%). AgZ used the ninth time almost had the same pore diameter distribution with that used the sixth

Table 2. Physical properties of zeolite composites.

Antibacterial materials		S_{BET}	Pore diameter distribution (%)		
		(m^2/g)	< 20 nm	20–80 nm	> 80 nm
Zeolite	Fresh	257	16.1	73.7	10.2
1 wt% AgZ	Fresh	216	14.5	78.1	7.4
	Run 6 (6th recycle)	115	8.9	30.3	60.8
	Run 9 (9th recycle)	106	8.3	30.3	61.4

S_{BET}: Brunauer-Emmett-Teller specific surface area.

time. It could be found that the pore diameter size of AgZ was increased after antibacterial reaction which might be due to bioaerosols blocking the smaller pores.

Effect of Zeolite and AgZ on Antibacterial Efficiency

Under the experimental conditions of bacterium and fungus initial concentrations were 1,215 ± 348 and 983 ± 352 CFU/m^3 (N = 20) in the 100 m^3 room. To evaluate the influence of Ag coated into zeolite composites on antibacterial efficacies, the experiments of AgZ against bacterium and fungus were investigated. Fig. 4 and Fig. 5 detailed the antibacterial efficiencies of the 10 g AgZ composites against bacterium and fungus, and the results demonstrated that low and unstable antibacterial efficiency was exhibited of zeolite alone. As shown in Fig. 4, the antibacterial efficiencies of zeolite against bacterium had an unstable variation with time due to zeolite only having an adsorption removal mechanism but not having any significant antibacterial reaction. Zeolite has high capture capacity due to the properties of porosity resulting in high surface area. Zeolite could remove bioaerosols by the capture process, but they could also provide a favorable environment for bioaerosols to grow. We consider that zeolite only is not an effective antibacterial material without impregnating with Ag, but zeolite offers a better reservoir for Ag supported on it due to its channel structure. Although the antibacterial efficiencies of zeolite against fungus increased with operation time, the lower antibacterial efficiencies were 46, 58 and 63% for 30, 60 and 120 min. The results exhibit that antibacterial efficiencies of AgZ against bacterium and fungus were significantly raised to the 90% level, and all the antibacterial efficiencies were higher than that of zeolite alone. It was observed that the antibacterial efficiencies of 1 wt% AgZ against bacterium were 83%, 95% and 99% for 30, 60 and 120 min. As shown in Fig. 5, the antibacterial efficiencies of 1 wt% AgZ against fungus were 86%, 96% and 99% for 30, 60 and 120 min. The antibacterial efficiencies of AgZ against bacterium and fungus rapidly increased as the time increased from 0 to 15 min. The results demonstrate that AgZ had higher antibacterial efficiency (exceeding 30 and 40% for bacterium and fungus) than zeolite alone after 120 min operation. Comparing the antibacterial efficiencies of 1, 2 and 3 wt% AgZ, it could be found that there was less than 10% difference in antibacterial efficiency after 15 min operation. As shown in Fig. 4 and Fig. 5, the antibacterial efficiencies of 1, 2 and 3 wt% AgZ against bacterium and

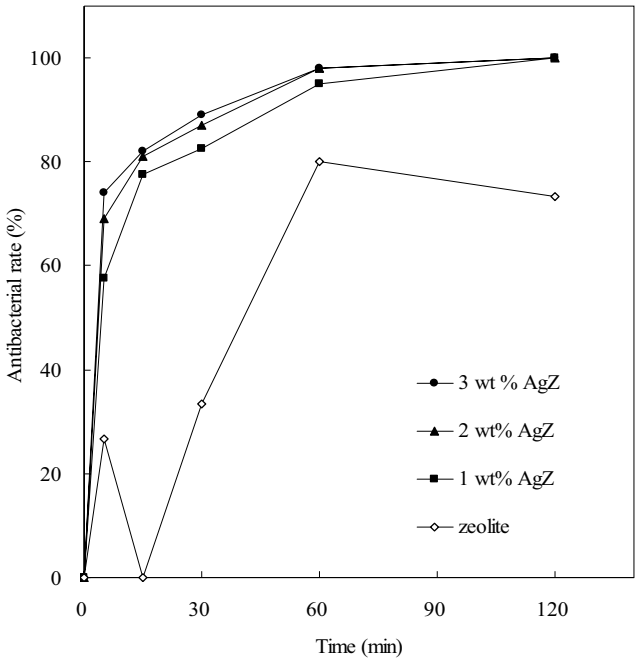

Fig. 4. The antibacterial efficiencies of zeolite composites against bacterium at different times. Condition: bacterium initial concentration was 1,215 ± 348 CFU/m^3 (N = 20).

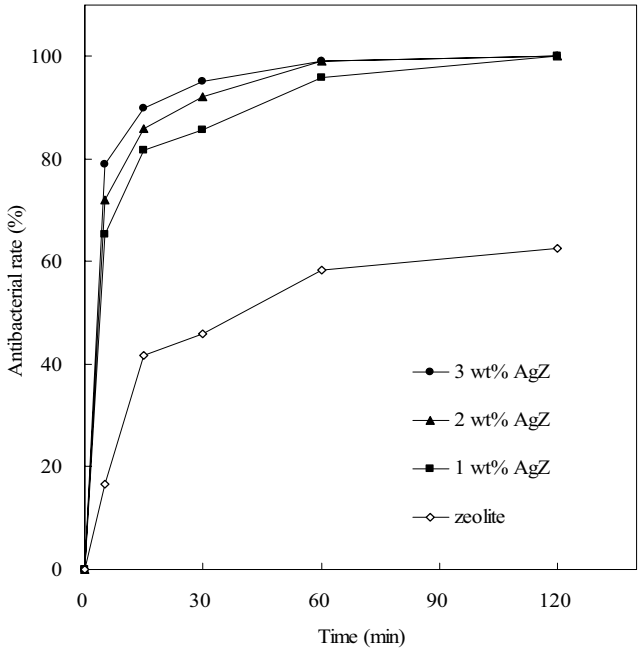

Fig. 5. The antibacterial efficiencies of zeolite composites against fungus at different times. Condition: fungus initial concentration was 983 ± 352 CFU/m^3 (N = 20).

fungus ranged from 78 to 82% and 82 to 90% after 15 min operation. Significant antibacterial efficiency took place in about 120 min, and the antibacterial efficiencies of 1, 2 and 3 wt% AgZ against bacterium and the fungus were all higher than 95%. According to this result, 1 wt% AgZ was considered to be more cost-effective. The results could show that zeolite coated with silver ions show better antibacterial efficiency against bacterium and fungus. Zeolite micropores offer unique reaction fields for catalytic reactions based on narrow pore, a variety of channel structure, a silver ion exchangeability and strong solid structure. The particle size of bioaerosols is usually bigger than zeolite micropores and bioaerosol cannot enter the zeolite micropore. Thus, the antibacterial reaction may only occur at the surface of zeolite. This phenomenon could reduce the antibacterial effectiveness factor for Ag. Therefore, it can be concluded that excessive silver impregnated on zeolite does not significantly increase the antibacterial efficiency. Furthermore, a relatively low bioaerosol concentration occurred in the indoor may also lead to excessive silver does not significantly increase the antibacterial efficiency. We consider that 1 wt% AgZ is the optimum material used in indoor environment. The high antibacterial efficiencies were due to bacterium being destroyed by the silver ions, and they include the following points: (1) the silver ions aid in the generation of reactive oxygen species, which are produced through the inhibition of respiratory enzymes by silver ions (Matsumura *et al.*, 2003); (2) the antibacterial activity of silver ions may also result from their ability for binding to essential enzyme sulfhydrals, thereby breaking these protein bonds (Oppermann *et al.*, 1980; Russell and Hugo, 1994).

Antibacterial Efficiency and Antibacterial Reaction Rate (k) of AgZ Regeneration

The antibacterial efficiencies of 1 wt% AgZ recycled and used during 10 and 80 hr were investigated by analyzing microbial counts. Antibacterial materials 1 wt% AgZ regenerated by a heating process (150°C, 2 h) before each recycled usage. The results are reported in Table 3, and the total bacterium and fungus counts in the influent of the fixed bed system were 3.7×10^4 to 8.6×10^4 CFU and 3.1×10^4 to 9.6×10^4 CFU during 10 hr, respectively. The 1 wt% AgZ had high and stable antibacterial efficiencies for nine recycle usages. As shown in Fig. 6 and Fig. 7, the average bacterium and fungus antibacterial efficiencies of each cycle were respectively higher than 93% (ranged from 93 to 98%) and 94% (ranged from 94 to 98%) after equilibrium. The total bacterium and fungus counts in the influent of the fixed bed system were 5.5×10^5 to 6.9×10^5 CFU and 4.4×10^5 to 5.8×10^5 CFU during 80 hr, respectively. We could find that bacterium and fungus antibacterial efficiencies were stable after 10 hr. The antibacterial efficiencies after 80 hr equilibrium operation of Fresh, Run 6 and Run 9 AgZ were respectively 94 ± 3, 94 ± 3 and 95 ± 3% for bacterium; and 94 ± 4, 92 ± 5 and 95 ± 2% for fungus. Each value of the mean and standard deviation were calculated from 24 data which were obtained after 80 hr operation.

The antibacterial reaction rate k_t was investigated to understand the AgZ antibacterial reaction rate in the indoor environment, and k_t also could be used as an indicator to evaluate the AgZ antibacterial ability with operation or regeneration times. The antibacterial reaction rates of 1 wt% AgZ during different 80 hr recycle operations were calculated and are presented in Fig. 8. The results show that the average bacterium antibacterial reaction rates of Fresh, Run 6 and Run 9 AgZ were respectively 856 ± 171, 706 ± 173 and 667 ± 165 CFU/g-hr; and the average fungus antibacterial reaction rates were 817 ± 136, 573 ± 160 and 547 ± 89 CFU/g-hr, respectively. Although the values of antibacterial reaction rates decreased with the times recycled, the value might also be affected by total microbial counts in the influent. In order to evaluate the AgZ antibacterial ability

Table 3. The antibacterial efficiency and maximum antibacterial capacity of AgZ.

Microbial information	Fresh	Run 2	Run 3	Run 4	Run 5	Run 6	Run 7	Run 8	Run 9
Bacterium removal for running 10 h									
N_0 (CFU)	8.6×10^4	8.2×10^4	3.7×10^4	5.2×10^4	7.4×10^4	8.4×10^4	7.0×10^4	6.6×10^4	7.0×10^4
q_T (CFU/g)	8.2×10^3	7.7×10^3	3.5×10^3	4.9×10^3	7.2×10^3	8.0×10^3	6.6×10^3	6.2×10^3	6.8×10^3
η_e (%)	98 ± 2	95 ± 5	93 ± 8	96 ± 4	97 ± 3	94 ± 1	97 ± 2	94 ± 3	96 ± 2
Fungus removal for running 10 h									
N_0 (CFU)	9.6×10^4	5.8×10^4	3.1×10^4	4.3×10^4	4.9×10^4	6.1×10^4	7.0×10^4	6.0×10^4	5.8×10^4
q_T (CFU/g)	9.2×10^3	5.5×10^3	3.0×10^3	4.1×10^3	4.7×10^3	5.9×10^3	6.6×10^3	5.8×10^3	5.6×10^3
η_e (%)	98 ± 2	95 ± 2	96 ± 4	95 ± 5	96 ± 3	95 ± 4	94 ± 3	96 ± 2	95 ± 2
Bacterium removal for running 80 h									
N_0 (CFU)	6.5×10^5	-	-	-	-	7.2×10^5	-	-	5.5×10^5
q_T (CFU/g)	6.1×10^4	-	-	-	-	6.9×10^4	-	-	5.3×10^4
η_e (%)	94 ± 3	-	-	-	-	94 ± 3	-	-	95 ± 3
Fungus removal for running 80 h									
N_0 (CFU)	5.8×10^5	-	-	-	-	4.5×10^5	-	-	4.4×10^5
q_T (CFU/g)	5.4×10^4	-	-	-	-	4.2×10^4	-	-	4.2×10^4
η_e (%)	93 ± 4	-	-	-	-	92 ± 5	-	-	95 ± 2

N_0: total microbial counts in influent.
q_T: total antibacterial capacity during the operation time.
η_e: antibacterial efficiency after equilibrium.

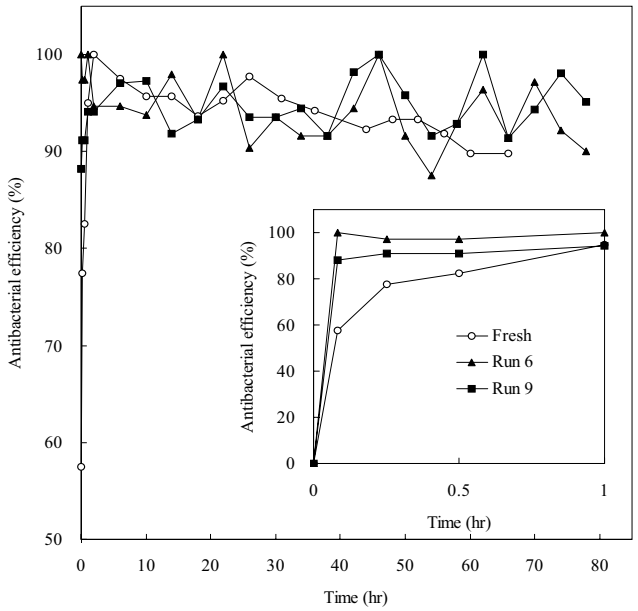

Fig. 6. The antibacterial efficiencies of fresh and reused AgZ against bacterium at different times.

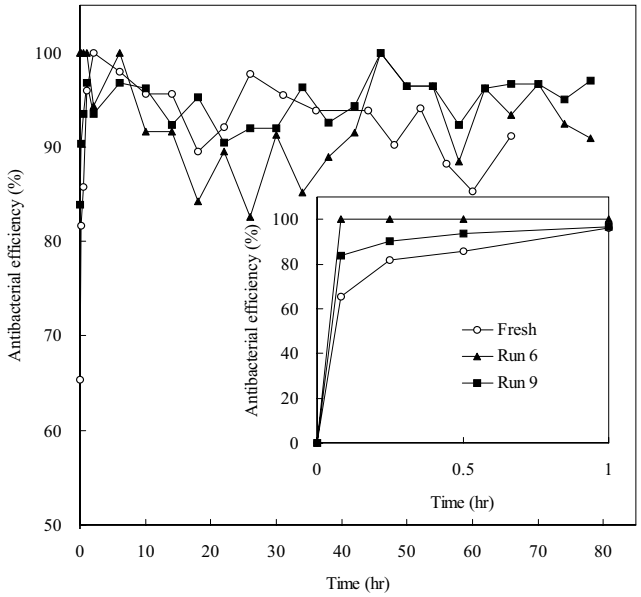

Fig. 7. The antibacterial efficiencies of fresh and reused AgZ against fungus at different times.

with operation or regeneration times, the coefficient of variation (CV) of AgZ k_t values was calculated. However, the CV value of the antibacterial reaction rate with the times recycled was relatively small (both bacterium and fungus were lower than 30%) in the antibacterial experiment. We could conclude that both bacterium and fungus were almost removed by 1 wt% AgZ. Combined with material regeneration technology, 1 wt% AgZ could continually be used nine times for 80 hr. To calculate the total use life-time, we could find that the efficient used time was more than 720 hr, and it could be seen that the process maintains high efficiency toward antibacterial reactions. The value of

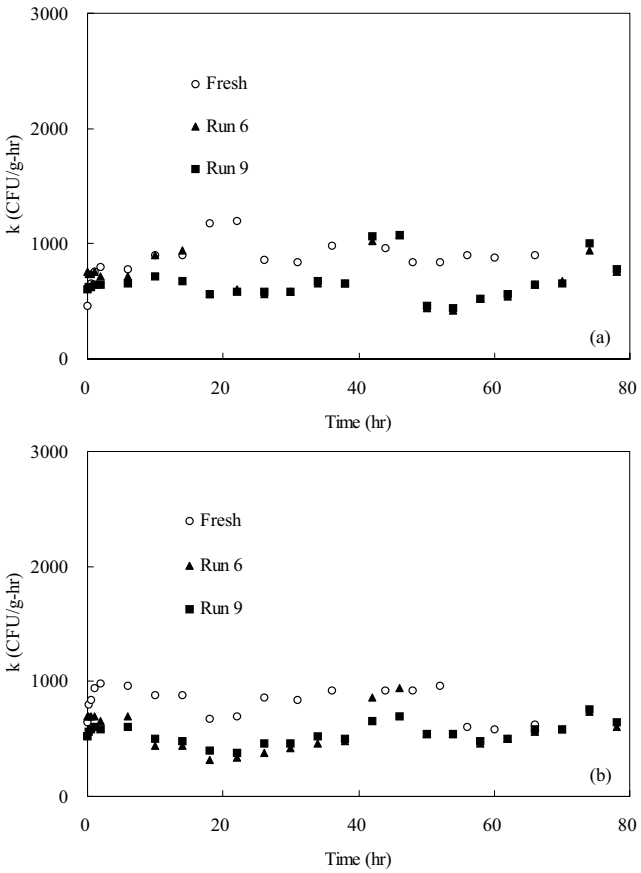

Fig. 8. Variations of (a) bacterium and (b) fungus antibacterial reaction rates of fresh and reused AgZ at different times.

k_t (CFU/g-hr) represents the kinetic parameter, and it can be defined as reaction rate constant.

The Total Antibacterial Capacity q_T of AgZ

To estimate q_T of AgZ (including fresh and regenerated AgZ) was one of the most important objects in this research. Establishing the value of q_T, the antibacterial ability of 1 wt% AgZ was understood. We used Eq. (2) to calculate the total antibacterial capacities over time, and the values are presented in Fig. 9 and Table 3. Because the microbial counts in the influent might affect the value of total antibacterial capacity, the relationship between them was investigated by linear regression (N = 24). The q_T values of bacterium and fungus ranged from 3.5×10^3 to 8.2×10^3 CFU/g and 3.0×10^3 to 9.2×10^3 CFU/g after 10 hr antibacterial reactions. The values of q_T after 10 hr antibacterial reactions were all lower than 80 hr, because AgZ did not approach saturation after 10 hr operation. As shown in Fig. 10, q_T had a positive relationship with the microbial counts in the influent when bacterium and fungus concentrations were 1,311 ± 368 and 1,049 ± 299 CFU/m^3, respectively. The bacterium and fungus q_T of 10 g AgZ used in a 100 m^3 room were at the least 6.9×10^4 CFU/g and 5.4×10^4 CFU/g, respectively. The values of both bacterium and fungus q_T could be considered as a limited value (maximum value) of the antibacterial capacity and be further used to estimate the life-time of AgZ.

The antibacterial reactions were conducted in a small-

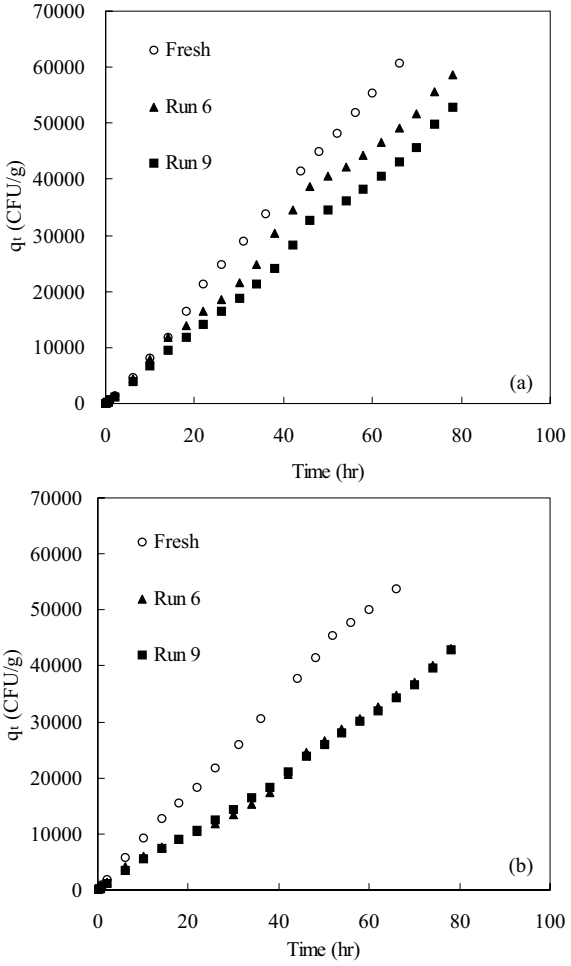

Fig. 9. The total adsorption capacity of (a) bacterium and (b) fungus onto fresh and reused AgZ at different times.

scale device with continuous air flow and thereby we can focus on the antibacterial characteristics of AgZ. The data obtained from this study could be applied in a larger device with relatively high flow rate as the amount of AgZ increases. The scale-up parameters for AgZ column include antibacterial reaction rate kt (CFU/g-hr) and total antibacterial capacity q_T (CFU/g). However, the operational parameters and the design of air ventilation system need to be considered. Moreover, further studies such as bioaerosol distribution in impactor stages of $PM_{10}/Pm_{2.5}/PM_1/PM_{0.5}$ (Furuuchi *et al.*, 2010) and user influence on indoor aerosol model (Hussein *et al.*, 2011) will be required to assure the value and improvement of this study.

CONCLUSIONS

AgZ nano-composite was successfully synthesized by a two-step method that included Y-type zeolites synthesis and Ag ion-exchange. Following this synthesis technology, 106–216 m^2/g surface area of AgZ was produced which could directly be applied in air conditioners. Antibacterial investigations demonstrated that AgZ could efficiently remove bioaerosols in indoor environments, and 1, 2 and 3 wt% AgZ significantly had higher antibacterial efficiencies (exceeded 30 and 40% for bacterium and fungus) than zeolite alone after 120 min operation. Bacterium and the fungus antibacterial efficiencies of 1, 2 and 3 wt% AgZ were all higher than 95%, and it could be considered that 1 wt% AgZ was more cost-effective. 1 wt% AgZ had relatively rapid antibacterial reaction (approached 90% antibacterial efficiency in 60 min) due to the Ag coated into zeolite, and it had excellent reused characteristics since when combining it with material regeneration technology, it could continually be used 80 hr for nine times (total life-time was more than

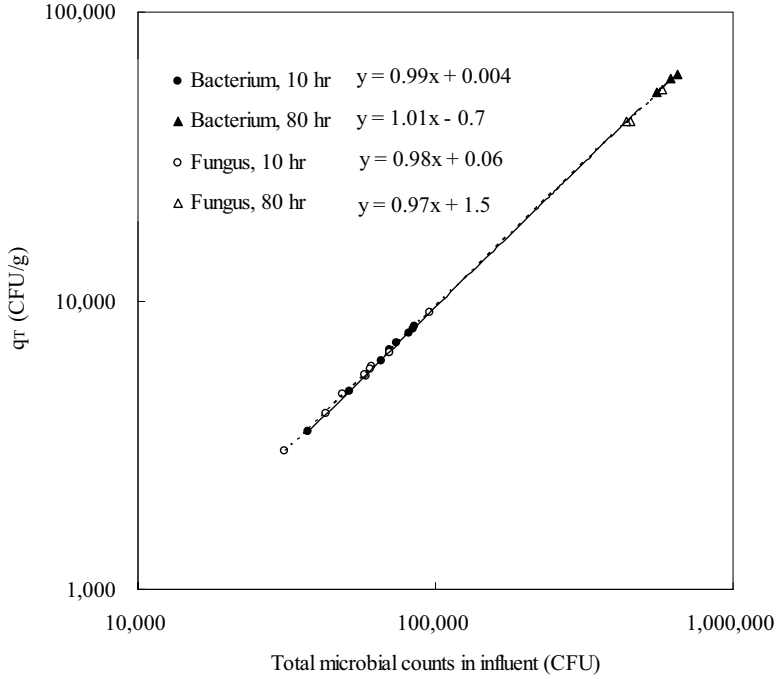

Fig. 10. Dependence of total microbial counts in influent on antibacterial capacity of AgZ.

720 hr). The values of k_t and q_T could be used as the operational parameters to calculate and design the amount of AgZ in future IAQ improvement.

ACKNOWLEDGMENTS

The authors gratefully acknowledge the financial support provided by the Ministry of Economic Affairs, R.O.C. (98-EC-17-A-10-S1-113).

REFERENCES

Cinar, C., Ulusu, T., Ozçelik, B., Karamüftüoğlu, N. and Yücel, H. (2009). Antibacterial Effect of Silver-zeolite Containing Root-canal Filling Material. *J. Biomed. Mater. Res. Part B* 90: 592–595.

Dastanian, M. and Seyedeyn-Azad, F. (2010). Desulfurization of Gasoline over Nanoporous Nickel-loaded Y-type Zeolite at Ambient Conditions. *Ind. Eng. Chem. Res.* 49: 11254–11259.

Duthie, M.S., Kimber, I. and Norval, M. (1999). The Effects of Ultraviolet Radiation on the Human Immune System. *Br. J. Dermatol.* 140: 995–1009.

Feng, Q.L., Wu, J., Chen, G.Q., Cui, F.Z., Kim, T.N. and Kim, J.O. (2000). A Mechanistic Study of the Antibacterial Effect of Silver Ions on Escherichia Coli and Staphylococcus Aureus. *J. Biomed. Mater.* 52: 662–668.

Furuuchi, M., Eryu, K., Nagura, M., Hata M., Kato, T., Tajima, N., Sekiguchi, K., Ehara, K., Seto, T. and Otani, Y. (2010). Development and Performance Evluation of Air Sampler with Inertial Filter for Nanoparticle Sampling. *Aerosol Air Qual. Res.* 10: 185–192.

Grinshpun, S.A., Adhikari, A., Honda, T., Kim, K.Y., Toivola, M., Rao, R.K.S. and Reponen, T. (2007). Control of Aerosol Contaminants in Indoor Air: Combining the Particle Concentration Reduction with Microbial Inactivation. *Environ. Sci. Technol.* 41: 606–612.

Huang, R., Agranovski, I., Pyankov, O. and Grinshpun, S. (2008). Removal of Viable Bioaerosol Particles with a Low-efficiency HVAC Filter Enhanced by Continuous Emission of Unipolar Air Ions. *Indoor Air* 18: 106–112.

Hussein, U., Molgaard B., and Hameri, K. (2011). User Influence on Indoor Aerosol Model Calibration. *Aerosol Air Qual. Res.* 11: 309–314.

Inoue, Y., Hoshino, M., Takahashi, H., Noguchi, T., Murata, T., Kanzaki, Y., Hamashima, H. and Sasatsu, M. (2002). Bactericidal Activity of Ag-zeolite Mediated by Reactive Oxygen Species under Aerated Conditions. *J. Inorg. Biochem.* 92: 37–42.

Inoue, Y., Kogure, M., Matsumoto, K., Hamashima, H., Tsukada, M., Endo, K. and Tanaka, T. (2008). Light Irradiation is a Factor in the Bactericidal Activity of Silver-loaded Zeolite. *Chem. Pharm. Bull.* 56: 692–694.

Jeon, H.J., Yi, S.C. and Oh, S.G. (2003). Preparation and Antibacterial Effects of Ag-SiO_2 Thin Films by Sol-gel Method. *Biomaterials* 24: 4921–4928.

Ji, J.H., Bae, G.N., Yun, S.H., Jung, J.H., Noh, H.S. and Kim, S.S. (2007). Evaluation of a Silver Nanoparticle Generator Using a Small Ceramic Heater for Inactivation of S. Epidermidis Bioaerosols. *Aerosol Sci. Technol.* 41: 786–793.

Jung, J.H., Oh, H.C., Noh, H.S., Ji, J.H. and Kim, S.S. (2006). Metal Nanoparticle Generation Using a Small Ceramic Heater with a Local Heating Area. *J. Aerosol Sci.* 37: 1662–1670.

Kawahara, K., Tsuruda, K., Morishita, M. and Uchida, M. (2000). Antibacterial Effect of Silver-zeolite on Oral Bacteria under Anaerobic Conditions. *Dent. Mater.* 16: 452–455.

Khanna, P.K., Singh, N., Charan, S. and Viswanath, A.K. (2005). Synthesis of Ag/Polyaniline Nanocomposite via an in Situ Photo-redox Mechanism. *Mater. Chem. Phys.* 92: 214–219.

Kim, H.J., Kim, S.S., Lee, Y.G. and Song, K.D. (2010). The Hydric Performance of Moisture Adsorbing/Desorbing Building Materials. *Aerosol Air Qual. Res.* 10: 625–634.

Kwon., S.b., Kim, S., Park, D.S., Cho, Y., Kim, J, Kim, M. and Kim, T. (2011). Novel Air Filtration Device for Building Air Handling Unit. *Aerosol Air Qual. Res.* 11: 570–577.

Lee, B.U. (2011). Life Comes from the Air: A Short Review on Bioaerosol Control. *Aerosol Air Qual. Res.* 11: 921–927.

Lee, B.U., Hong, I.G., Lee, D.H., Chong, E.S., Jung, J.H., Lee, J.H., Kim, H.J., and Lee, I.S. (2011). Bacterial Bioaerosol Concentrations in Public Restroom Environments. *Aerosol Air Qual. Res.* 12: 251–255.

Lin, C.Y. and Li, C.S. (2002). Control Effectiveness of Ultraviolet Germicidal Irradiation on Bioaerosols. *Aerosol Sci. Technol.* 36: 474–478.

Main, C.E. (2003). Aerobiological, Ecological, and Health Linkages. *Environ. Int.* 29: 347–349.

Matsumura, Y., Yoshikata, K., Kunisaki, S. and Tsuchido, T. (2003). Mode of Action of Silver Zeolite and Its Comparison with that of Silver Nitrate. *Appl. Environ. Microbiol.* 69: 4278–4281.

Mohan, R., Shanmugharaj, A.M. and Hun, R.S. (2011). An Efficient Growth of Silver and Copper Nanoparticles on Multiwalled Carbon Nanotube with Enhanced Antimicrobial Activity. *J. Biomed. Mater. Res. Part B* 96: 119–126.

Morrison, M.L., Buchanan, R.A., Liaw, P.K., Berry, C.J., Brigmon, R.L., Riester, L., Abernathyd, H., Jind, C. and Narayan, R.J. (2006). Electrochemical and Antimicrobial Properties of Diamondlike Carbon-metal Composite Films. *Diamond Relat. Mater.* 15: 138–146.

Nicas, M. and Miller, S.L. (1999). A Multi-zone Model Evaluation of the Efficacy of Upper-room Air Ultraviolet Fermicidal Irradiation. *Appl. Occup. Environ. Hyg.* 14: 317–328.

Oppermann, R.V., Rolla, G., Johansen, J.R. and Assev, S. (1980). Thiol Groups and Reduced Acidogenicity of Dental Plaque in the Presence of Metal Ions in Vivo. *Scand. J. Dent. Res.* 88: 389–396.

Park, H.J., Kim, Y.Y., Kim, J., Lee, J.H., Hahn, J.S., Gu, M.B. and Yoon, J. (2009). Silver-ion-mediated Reactive Oxygen Species Generation Affecting Bacterial Activity.

Water Res. 43: 1027–1032.

Paschoalino, M.P. and Jardim, W.F. (2008). Indoor Air Disinfection Using a Polyester Supported TiO_2 Photoreactor. *Indoor Air* 18: 473–479.

Phillips, T.J., Bloudoff, D.P., Jenkins, P.L. and Stroud, K.R. (1999). Ozone Emissions from a "Personal Air Purifier". *J. Exposure Anal. Environ. Epidemiol.* 9: 594–601.

Reynolds, S.J., Black, D.W., Borin, S.S., Breuer, G., Burmeister, L.F., Fuortes, L.J., Smith, T.F., Stein, M.A., Subramanian, P., Thorne, P.S. and Whitten, P. (2001). Indoor Environmental Quality in Six Commercial Office Buildings in the Midwest United States. *Appl. Occup. Environ. Hyg.* 16: 1065–1077.

Ruihong, Z., Fen, G., Yongqi, H. and Huanqi, Z. (2006). Self-assembly Synthesis of Organized Mesoporous Alumina by Precipitation Method in Aqueous Solution. *Microporous Mesoporous Mater.* 93: 212–216.

Russell, A.D. and Hugo, W.B. (1994). Antimicrobial Activity and Action of Silver. *Prog. Med. Chem.* 31: 351–370.

Srikanth, P., Sudharsanam, S. and Steinberg, R. (2008). Bioaerosols in Indoor Environment: Composition, Health Effects and Analysis. *Indian J. Med. Microbiol.* 26: 302–312.

Talebi, J., Halladj, R. and Askari, S. (2010). Sonochemical Synthesis of Silver Nanoparticles in Y-zeolite Substrate. *J. Mater. Sci.* 45: 3318–3324.

Thom, D.C., Davies, J.E., Santerre, J.P. and Friedman, S. (2003). The Hemolytic and Cytotoxic Properties of a Zeolite-containing Root Filling Material in Vitro. *Oral. Surg. Oral. Med. O.* 95: 101–108.

Tringe, S.G., Zhang, T., Liu, X., Yu, Y., Lee, W.H., Yap, J., Yao, F., Suan, S.T., Ing, S.K., Haynes, M., Rohwer, F., Wei, C.L., Tan, P., Bristow, J., Rubin, E.M. and Ruan, Y. (2008). The Airborne Metagenome in an Indoor Urban Environment. *PLoS ONE.* 3: 1–10.

Wang, Y., Xu, X., Tian, Z., Zong, Y., Cheng, H. and Lin, C. (2006). Selective Heterogeneous Nucleation and Growth of Size-controlled Metal Nanoparticles on Carbon Nanotubes in Solution. *Chem. Eur. J.* 12: 2542–2549.

Wu, K.H., Chang, Y.C., Zheng, M.Z., Yang, C.C. and Lin, W.P. (2011). Preparation and Characterization of Ag-deposited Aminosilane-modified Silicate by Chemical Reduction Method. *J. Polym. Sci., Part B: Polym. Phys.* 49: 566–573.

Zhang, S., Fu, R., Wu, D., Xu, W., Ye, Q. and Chen, Z. (2004). Preparation and Characterization of Antibacterial Silver-dispersed Activated Carbon Aerogels. *Carbon* 42: 3209–3216.

Zhang, Z.Y., Shi, T.B, Jia, C.Z., Ji, W.J., Chen, Y. and He, M.Y. (2008). Adsorptive Removal of Aromatic Organosulfur Compounds over the Modified Na-Y Zeolites. *Appl. Catal., B* 82: 1–10.

Received for review, August 24, 2011
Accepted, February 6, 2012